Portability of TV-Regularized Reconstruction Parameters to Varying Data Sets

Mario Amrehn[1], Andreas Maier[1,2], Frank Dennerlein[1], Joachim Hornegger[1,2]

[1]Pattern Recognition Lab, FAU Erlangen-Nürnberg
[2]Erlangen Graduate School in Advanced Optical Technologies (SAOT)
`mario.amrehn@fau.de`

Abstract. In C-arm computed tomography there are certain constraints due to the data acquisition process which can cause limited raw data. The reconstructed image's quality may significantly decrease depending on these constraints. To compensate for severely under-sampled projection data during reconstruction, special algorithms have to be utilized, more robust to such ill-posed problems. In the past few years it has been shown that reconstruction algorithms based on the theory of compressed sensing are able to handle incomplete data sets quite well. In this paper, the iterative iTV reconstruction method by Ludwig Ritschl et al. is analyzed regarding it's elimination capabilities of image artifacts caused by incomplete raw data with respect to the settings of it's various parameters. The evaluation of iTV and the data dependency of iterative reconstruction's parameters is conducted in two stages. First, projection data with severe angular under-sampling is acquired using an analytical phantom. Proper reconstruction parameters are selected by analyzing the reconstruction results from a set of proposed parameters. In a second step multiple phantom data sets are acquired with limited angle geometry and a small number of projections. The iTV reconstructions of these data sets are compared to short-scan FDK and SART reconstruction results, highlighting the distinct data dependence of the iTV reconstruction parameters.

1 Introduction

C-arm systems with a mounted X-ray tube and flat panel detector are very popular in medical image acquisition [1]. The C-arm device is typically rotated around the patient in a 200° radius or less. During rotation projection images are acquired and utilized for reconstructing a 3D distribution of the object's X-ray attenuation coefficients. Due to the limited projection angle of the C-arm and a small number of projections severe artifacts may show in the computed coefficients. Reconstructing from limited raw data, the very popular reconstruction method of Feldkamp-Davis-Kress (FDK) [2] does not yield optimal results. Iterative methods are designed to compensate those artifacts by iteratively alternating between backprojecting data into the reconstructed image and projecting intermediate reconstruction images back into the raw data domain. Especially

a combination of iterative algorithms with insights from Compressed Sensing [3] seems to improve reconstruction results from limited raw data [4]. The problem arising from those hybrid approaches is twofold. The runtime for a final solution to emerge may significantly increase. Furthermore, the number of parameters to be set by the user may be the sum of the combined method's free variables. This introduces a high dimensional optimization space. In the following, the impact of changes to the parameter set is analyzed.

2   Materials and methods

A method to solve the inverse problem of the Radon transform is to formulate the reconstruction problem as a system of linear equations. A reconstruction is performed minimizing an objective function which may incorporate prior knowledge about the image. One unconstrained objective function for an iterative reconstruction approach is defined by the SSD measure between the original projection values and the projected current image

$$\min ||R\,f(r) - p||_2^2 \tag{1}$$

where $f(r)$ is the value of voxel $r = (r_1, r_2, r_3)$ in the reconstructed image f. $R\,f(r)$ is the system of linear equations with X-ray transform R. p denotes the measured raw projection data.

2.1   Compressed sensing

Compressed Sensing is a signal processing technique to deal with the problem of incomplete data sets [3, 5] when reconstructing by finding solutions to underdetermined linear systems. It takes advantage of the signal's sparseness or compressibility in some domain, allowing the entire signal to be determined from relatively few measurements. This sparseness can be incorporated into a constraint. A signal is transformed by a sparsifying operator Ψ into a suitable domain for measuring it's compressibility. For a signal $f \in \mathbb{R}^n$ the transformation in an orthonormal basis is defined as $f(t) = \sum_i^n x_i \Psi_i(t)$, where x_i is the coefficient sequence of f, $x_i = \langle f, \Psi_i \rangle$ in the basis Ψ. With under-sampled data, only a subset of all n coefficients of f can be measured

$$y_k = \langle f, \phi_k \rangle, \quad k \in M \subset [1 \ldots n] \tag{2}$$

ϕ_k is the function discretizing f to samples y_k and may be a Dirac delta function shifted by k. The reconstruction is given by $\hat{f} = \Psi \hat{x}$ where $\hat{x}$ is the solution of the convex optimization

$$\min_{x_{\text{app}} \in \mathbb{R}^n} ||x_{\text{app}}||_{\ell 1} \text{ subject to } y_k = \langle \phi_k, \Psi_{x_{\text{app}}} \rangle \quad \forall k \in M \tag{3}$$

There may be multiple solutions for $\hat{f} = \Psi x_{\text{app}}$. The one is chosen which coefficient sequence minimizes the $\ell 1$ norm, a suitable measure for the function's sparsity. This also penalizes image artifact creation during reconstruction.

2.2   Simultaneous algebraic reconstruction technique (SART)

Starting from an initial guess for the reconstructed object, SART performs a sequence of iterative grid projections and correction back-projections until the reconstruction has converged [6]. An update of the current image is performed after all rays in one projection are processed. Correction terms are computed to update the image voxel values with respect to their objective function, then combined by a weighted sum

$$f_i^{\nu+1} = f_i^{\nu} + \beta \cdot \sum_{k \in s(\nu)} \frac{1}{\sum_j (R^T)_{i,j}^k} (R^T)_{i,j}^k \frac{\sum_i R_{j,i}^k f_i^{\nu} - p_j^k}{\sum_i R_{j,i}^k}, \; \nu \in [0, N_{\text{Sub}}[\quad (4)$$

where the system matrix $R_{i,j}^k$ of the k-th projection maps f on p^k. The index i represents an image voxel r. j is a projection's element. The relaxation parameter $\beta \in]0,1]$ controls the convergence speed of the minimization. The choice of the number of subsets N_{Sub} affects the angular distance between successively used projections. All elements of f_i are processed in each sub iteration ν [4]. Iterating over all subsets ν yields one full SART-iteration f_{n+1}^{SART}. SART has many advantages over FDK, such as better noise tolerance and handling of sparse and non-uniformly distributed projection datasets. However, computation time is considerably higher [6].

2.3   Constrained total variation optimization (TV)

With incomplete data the inverse problem to (1) is under-determined causing an infinite number of possible solutions for a reconstructed image. One proposed approach utilizes an iterative reconstruction combined with Compressed Sensing by extending the cost function with a constraint from a priori knowledge. The signal $f(r)$ can be completely reconstructed with a high probability with less samples than required by the Nyquist criterion, if most entries of $\Psi f(r)$ are zero i.e. a sparsifying transformation is known. This is approximated by the ℓ1-norm of $\Psi f(r)$ [4, 7] as seen in (3). This yields an inequality-constraint convex optimization function as a penalized least squares approach (Tikhonov regularization)

$$\min \|\Psi f(r)\|_1 \text{ subject to } \|R f(r) - p\|_2^2 < \epsilon \quad (5)$$

minimizing the raw data cost function with the sparsity constraint at a low value. To speed up the computation, iTV [4] minimizes the raw data cost function via SART and image sparsity separately in their own domain, using the image gradient ∇ as Ψ and a Gradient Descent approach, which in each of it's M steps reduces the cost function $\|\nabla f(r)\|_1$, called the total variation

$$f_{n+1,m+1}^{TV}(r) = f_{n+1,m}^{TV}(r) + \alpha \cdot \nabla \|\nabla f_{n+1,m}^{TV}(r)\|_1 \quad (6)$$

$$\nabla \|\nabla f_{n+1,m}^{TV}(r)\|_1 \approx \frac{(\nabla_{xx} f_{n+1,m}^{TV} + \nabla_{yy} f_{n+1,m}^{TV} + \nabla_{zz} f_{n+1,m}^{TV})}{\sqrt{(\nabla_x f_{n+1,m}^{TV})^2 + (\nabla_y f_{n+1,m}^{TV})^2 + (\nabla_z f_{n+1,m}^{TV})^2 + \text{regul}^2}}$$

$$(7)$$

Table 1. Default parameters for the iTV reconstruction and it's variations.

Type	β	ω	λ_{max}	eTV-Iterations	regul	α_{init}	GD-Iterations
Default	0.4	0.8	1.2	20	10^{-4}	0.3	25
Changes	0.8	0.4	$\{5, \infty\}$	$\{10, 30\}$	10^{-2}	0.8	10

The linear combination of the two resulting intermediate images form a full iTV iteration. An optimal parameter value $\lambda \in]0; 1]$ is determined in the raw data domain by solving the quadratic (9), since ϵ_{n+1} is known and ω is set by the user [4]

$$\epsilon_{n+1} = (1 - \omega) \cdot \|Rf_{n+1}^{SART}(r) - p\|_2^2 + \omega \cdot \epsilon_n, \quad \omega \in]0; 1[\tag{8}$$

$$\|R[(1 - \lambda)f_{n+1}^{SART}(r) + \lambda f_{n+1,M}^{TV}(r)] - p\|_2^2 = \epsilon_{n+1} \tag{9}$$

$$f_{n+1} = (1 - \lambda)f_{n+1}^{SART}(r) + \lambda f_{n+1,M}^{TV}(r) \tag{10}$$

3   Results

To evaluate the portability of a parameter set for iTV, a two-pass experiment is performed. In the first stage a proper parameter set for a given reconstruction problem is evaluated. In the second stage, the parameter set is used for different reconstruction scenarios as proposed in [8]. All reconstructions were computed on projection images corrupted with Poisson distributed noise and a simulated radiation dose of $k = 10^6$ X-ray photons.

On a circular trajectory of radius $750\,\mathrm{mm}$ with a detector-source distance of $1200\,\mathrm{mm}$, 227 projections are simulated on an angle of $170.25°$ with an angular increment of $.75°$. The detector's 800×800 pixel size is $6\,\mathrm{mm}$ in each dimension. The ground truth data is a $512 \times 512 \times 174$ centered version of the FORBILD head phantom with $6\,\mathrm{mm}$ regular hexahedron voxels. For the parameter search, a star-shaped pattern is chosen, i.e. from a default set only one parameter is altered prior to a new reconstruction run. After these ten reconstructions seen in Tab. 1 the best set is chosen by the RMSE, Pearson Correlation, MSSIM, PSNR, TV norm metrics as well as human inspection. The unambiguously best result comes from the default set plus relaxation parameter $\beta = 8$ In the second part, phantoms were reconstructed with limited angle and few projections through angular incrementation. Results for limited angle are presented in Tab. 2. Graphical results are presented in Fig. 1.

4   Discussion

The fixed set of parameters optimized for a limited angle acquisition of the FORBILD head phantom was used during reconstruction of various scenarios.

Table 2. Reconstruction results with limited angle relative to ground truth or FDK in percent. Left FORBILD head, right human head phantom.

		200°	185°	170°	155°	140°	200°	185°	170°	155°	140°
	RMSE	56.0	49.9	50.5	51.1	46.7	57.7	49.1	55.8	56.7	53.9
	PC	101.5	102.6	103.1	103.1	105.7	57.7	49.1	55.8	56.7	53.9
SART	MSSIM	96.7	89.9	100.9	113.5	124.1	99.2	108.5	118.1	122.4	134.2
	PSNR	155.7	171.8	156.0	163.6	208.7	141.5	145.2	140.5	148.4	147.3
	TVNORM	135.4	117.1	122.9	129.4	144.5	125.5	112.0	119.0	121.4	133.7
	RMSE	16.6	19.4	29.2	31.5	37.9	44.9	38.2	52.4	51.7	47.1
	PC	102.1	103.4	103.9	104.0	106.6	102.2	103.8	104.6	105.3	110.4
iTV	MSSIM	140.9	131.5	149.1	168.7	180.5	111.9	123.2	131.2	137.3	159.4
	PSNR	149.1	138.1	127.1	134.8	168.1	122.8	129.3	120.9	121.9	128.5
	TVNORM	57.2	49.9	46.1	45.8	47.8	40.8	35.6	29.4	29.8	34.2

4.1 Limited angle

For the FORBILD head phantom data and limited angle geometry, the SART and the iTV algorithm are superior to the short-scan FDK method in terms of the introduced error metrics, the RMSE in particular. The iTV reconstruction is superior to the SART method according to every metric except the Peak Signal-to-Noise Ratio causing more blurred transitions at the inner boundaries

| | $\Theta_{\mathrm{max}} = 155°$ | $\Theta_{\mathrm{max}} = 155°$ | $\Theta_{\Delta} = 2.25°$ | $\Theta_{\Delta} = 2.25°$ |
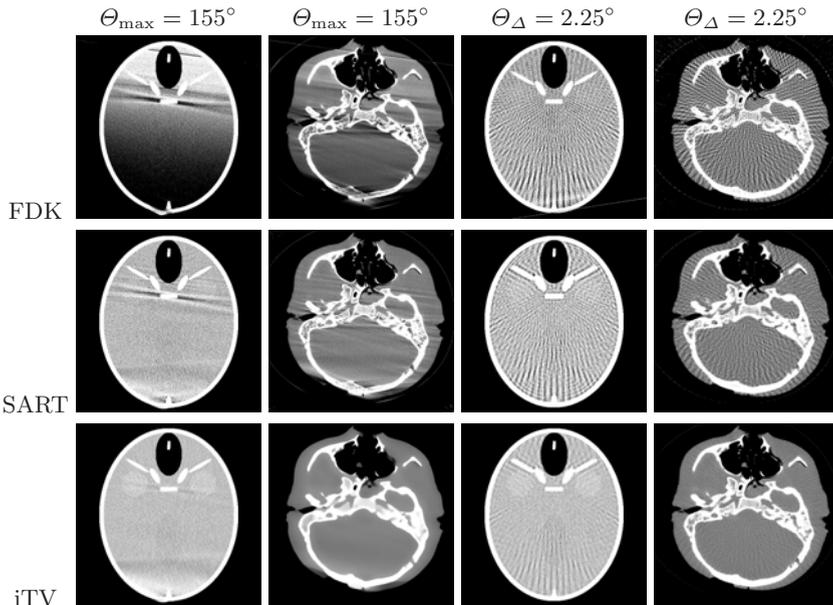
Fig. 1. FORBILD head phantom and human head phantom with limited angle ($\Theta_{\mathrm{max}} = 155°$) and few projections ($\Theta_{\Delta} = 2.25°$). WC:0, WW:$\{200, 1000\}$.

of the object. The inhomogeneous regions resulting from the X-ray photon noise induced and streak artifacts are less prominent in iTV improving the perception of low contrast elements. However, the porous bone structure of the human head phantom got blurred significantly using the same set of parameters for this reconstruction.

4.2   Few projections

According to the error metrics, there is a clear hierarchy in the assessment of data quality with few projections. The RMSE of the iTV method is less than half the SART's. Elements with small changes in their attenuation coefficients are better preserved and not partially overlayed by streaks. For the FORBILD head phantom iTV performs a superior preservation of resolution. Again, more structure is lost in the human head phantom reconstruction. Altogether, iTV handles under-sampled data due to a high angular increment over a short-scan acquisition procedure quite well. However, it becomes apparent that a proper parameter set for limited angle may not be transferable to different geometries without a loss in quality.

References

1. Dennerlein F. Image Reconstruction from Fan-Beam and Cone-Beam Projections. Universitätsverlag Erlangen; 2008.
2. Feldkamp L, Davis L, Kress J. Practical cone-beam algorithm. J Opt Soc Am A. 1984;1(6):612–9.
3. Donoho DL. Compressed sensing. IEEE Trans Inf Theory. 2006;52(4):1289–306.
4. Ritschl L, Bergner F, Fleischmann C, et al. Improved total variation-based CT image reconstruction applied to clinical data. Phys Med Biol. 2011;56(6):1545.
5. Wu H, Maier A, Fahrig R, et al. Spatial-temporal total variation regularization (STTVR) for 4D-CT reconstruction. Proc SPIE. 2012; p. 83133J.
6. Mueller K. Fast and Accurate Three-Dimensional Reconstruction from Cone-Beam Projection Data Using Algebraic Methods. The Ohio State University; 1998.
7. Chambolle A. An algorithm for total variation minimization and applications. J Math Imaging Vis. 2004;20(1-2):89–97.
8. Amrehn M. Implementation and Evaluation of a Total Variation Regularized Iterative CT image Reconstruction Method. Friedrich-Alexander-University Erlangen-Nürnberg; 2014.